

Research



Cite this article: Plitman Mayo R, Abbas Y, Charnock-Jones DS, Burton GJ, Marom G. 2019 Three-dimensional morphological analysis of placental terminal villi. *Interface Focus* **9**: 20190037.
<http://dx.doi.org/10.1098/rsfs.2019.0037>

Accepted: 15 May 2019

One contribution of 15 to a theme issue 'Bioengineering in women's health, volume 2: pregnancy—from implantation to parturition'.

Subject Areas:

bioengineering, biomechanics

Keywords:

morphology, placenta, terminal villi, three-dimensional reconstruction, confocal laser scanning microscopy

Author for correspondence:

Romina Plitman Mayo
e-mail: rominap@mail.tau.ac.il

Three-dimensional morphological analysis of placental terminal villi

Romina Plitman Mayo¹, Yassen Abbas^{2,3}, D. Stephen Charnock-Jones^{2,4}, Graham J. Burton² and Gil Marom¹

¹School of Mechanical Engineering, Tel Aviv University, Tel Aviv, Israel

²Centre for Trophoblast Research (CTR), Department of Physiology, Development and Neuroscience, University of Cambridge, Cambridge CB2 3EG, UK

³Department of Pathology, University of Cambridge, Cambridge CB2 1QP, UK

⁴Department of Obstetrics and Gynaecology, University of Cambridge, Cambridge CB2 0SW, UK

RPM, 0000-0002-3013-0717; GM, 0000-0003-3130-3402

Transport of nutrients and waste between the maternal and fetal circulations during pregnancy takes place at the final branches of the placental villous trees. Therefore, and unsurprisingly, pregnancy complications have been related to the maldevelopment of terminal villi. However, a deep analysis of placental villous morphology has been limited by tissue processing and imaging techniques. In this proof-of-principle study, placental lobules were fixed by perfusion and small clumps of villi were stained, sectioned optically and reconstructed. Morphological and network analyses were suggested and demonstrated on samples of normal placentas. The results show that most parameters are almost constant within a placenta but that there exists an inter-individual variation. Network analysis suggests that the fetoplacental capillary network has several paths within an individual villus, serving as an efficient transport system. Three-dimensional reconstruction from confocal laser scanning microscopy images is a potent technique able to quantify placental architecture and capture the significant irregularities in vessel diameter and membrane thickness. This approach has the potential to become a powerful tool to further our understanding of the differences in placental structure which may underlie pregnancy complications.

1. Introduction

The placenta is the organ that interfaces between the mother and her developing baby. Among its several functions, the exchange of respiratory gases is perhaps the most critical for achieving a successful pregnancy. Therefore, several studies attempted to quantify the placental structural features that are involved in gas transfer [1–3]. Human placental gas transport takes place in the final branches of the villous tree, commonly referred to as the terminal villi, due to their high vascularity and the thin membrane separating the maternal and fetal bloodstreams [4].

The morphology of the terminal villi has been widely studied due to its importance for adequate fetal development [5–9]. Inside the villi, the fetal capillaries are tortuous and have variable diameters, sharp bends and different types of loops [10]. Parameters of interest include the surface area available for exchange, volumetric ratios and membrane arithmetic and harmonic mean thicknesses. These have been calculated in normal and diseased placentas, showing remarkable differences between them [3,11–22]. For example, by analysing capillarization, villous maturation and capillary lumen remodelling of peripheral villi, Mayhew *et al.* [16] concluded that fetal growth restriction (FGR), but not pre-eclampsia (PE), is associated with poor villous development and fetoplacental angiogenesis. However, a later study by Egbor *et al.* [19] found that, although terminal villi from late-onset PE placentas were morphologically similar to matched controls, those from early-onset PE were significantly different, suggesting that the later state is a placental disorder. The impact of maternal diabetes mellitus (DM) on the development of terminal villi has also been the subject of several investigations: type 1

DM was found to increase the surface area of the fetoplacental capillary network by elongation and enlargement of the vessel diameter [23]; type 2 DM showed abnormal branching patterns, with either hypo- or hyper-ramifications [12]. Gestational diabetes (GD) leads to an expansion of the villous membrane by increasing the villous diameter, while reducing the capillary diameter. Clearly, a deep morphological analysis of the capillary bed and its arrangement within the terminal villi is of major importance to better understand transport processes in the human placenta.

Different research techniques have emerged in the last century to better assess the micro-structure of the human placenta. One of the earliest and perhaps the most accurate approach was employed by Kaufmann *et al.* [5,7] and Sen *et al.* [6], who aspirated villi directly into fixative from the *in situ* placenta during a caesarean operation; unfortunately, this method is no longer in use. Nowadays, only delivered placentas can be sampled and the tissue requires rapid fixing to avoid vascular collapse and allow further processing. The different fixation techniques provide adequate results; however, perfusion fixation has been shown to restore the *in vivo* state [1]. Further processing of fixed tissue can lead to two-dimensional (2D) histological sections [1,5,16], three-dimensional (3D) vascular casts [7,11] or 3D confocal laser scanning microscopy (CLSM) image stacks [10,24–27]. Stereological techniques applied to histological sections are currently the most common approach to estimate 3D values based on 2D images. With this approach, one obtains unbiased estimates of vessel density, volume and surface fractions, villous and vessel diameters and membrane thickness [1]. However, 2D images have been shown to inaccurately represent some of these parameters due to the complex architecture of the fetoplacental capillary network [28]. Three-dimensional reconstructions from fluorescent CLSM image stacks are becoming an alternative powerful tool to visualize and quantify terminal villous structure [29].

The aim of this study is to quantify the spatial arrangement and complexity of the terminal villi and their capillary beds in normal placentas using 3D reconstructions. To this end, terminal villi from perfused placentas were immunolabelled, optically scanned and reconstructed. These reconstructions were used to quantify structural parameters and to understand the complicated transport networks in the human placenta.

2. Material and methods

2.1. Specimen preparation

Three fresh healthy placentas delivered by caesarean section at term were obtained at the Department of Obstetrics & Gynaecology at the Rosie Hospital, Cambridge, UK, with ethics permission and informed written consent. Undamaged and clot-free peripheral lobules suitable for perfusion fixation [1] were identified; the supplying chorionic artery was cannulated and the draining vein was cut to allow free flow of perfusate. Fetal blood was cleared from the lobules with phosphate-buffered saline (PBS). The lobules were then fixed by perfusion with 10% formalin (approx. 20 min) followed by removal with PBS (an additional 20 min). Two lobules were fixed from placenta 1 at pressures of 100 mmHg (samples 1 and 2) and 30 mmHg (samples 3 and 4) [10]. A single lobule was perfused from placenta 2 and placenta 3 at 40 mmHg. The fixed lobules were then immersed in 10% formalin for 48 h to fix the trophoblast bilayer.

The fetoplacental vessels in the first four samples (placenta 1) were stained by perfusion with green fluorescein isothiocyanate (FITC) conjugated *Ulex* lectin (FL-1061; Vector Laboratories, Peterborough, UK) diluted in PBS. Small samples were dissected with needles, and randomly selected samples were incubated for 10 min in DiI (D-282; Thermo Fisher Scientific, MA, USA) to stain the villous membranes; these samples were used in previous studies [10,27]. The remaining eight samples (placentas 2 and 3) were dissected and washed with PBS before being permeabilized by tris-buffered saline (TBS) containing 0.1% Triton X-100 for 30 min and blocked with TBS 0.1% Triton X-100 + 2% goat serum for 30 min. The villous membrane and endothelial layer of the terminal villi were immunolabelled with a mixture of anti-cytokeratin 7 (1 : 50; M7018; Agilent Technologies, Santa Clara, CA, USA) and *Ulex* lectin (1 : 200; L8262; Sigma-Aldrich, St Louis, MO, USA) diluted in PBS + 2% goat serum. The samples were incubated overnight at 4°C. Thereafter, the samples were washed thoroughly (five times) with TBS and incubated for 1 h at room temperature in streptavidin conjugated with Alexa488 and goat-anti-mouse IgG coupled with Alexa568 (Thermo Fisher Scientific, MA, USA). Lastly, the samples were washed five times in TBS and mounted on a 35 mm glass-bottomed dish (Ibidi, Martinsried, Germany) with a drop of Vectashield antifade mounting medium with DAPI (H-1200; Vector Laboratories, Peterborough, UK).

The first four samples (placenta 1) were scanned using a Leica SP2 CLSM (Leica Microsystems, Wetzlar, Germany) with a $\times 25$, 0.95NA objective lens. The remaining samples were imaged using a Zeiss LSM 700 (Zeiss, Oberkochen, Germany) with a $\times 20$ objective lens. Each image stack was approximately $250 \times 250 \times 250 \mu\text{m}^3$.

2.2. Geometry reconstruction

The geometrical reconstruction of the first four samples (placenta 1) is documented in a previous study [10]. The z-stacks of the remaining eight samples were processed in Amira 6.7 (Thermo Fisher Scientific, MA, USA), a software for advanced image processing and quantification. The CLSM stacks were segmented using the thresholding method [30]; resultant voids within the segmented area were filled using the *fill holes* module while segmented pixels outside of the desired area were removed by employing the *remove islands* module. Thereafter, a smoothing algorithm was applied per slice and for the whole volume. In order to overcome the poor z-resolution, the segmented stack was re-sampled to allow for an isotropic voxel size and a 3D facet-based surface was created for each sample using the *generate surface* module.

2.3. Morphological analysis

The first step to obtain the skeleton of the fetoplacental vascular networks is to calculate a distance map from the segmented stack. In a distance map, the value of each voxel is equal to the shortest distance to a border voxel. This map is then used to guide the *thinner* module, which computes a one-voxel-thick skeleton located at the centre of the segmented stack. The distance map is then evaluated at each point of the skeleton and the shortest distance is taken as the thickness or as the smallest possible radius. An example of this procedure is shown in figure 1.

Several basic morphological parameters were calculated using the *Spatial Graph Statistics* module in the image processing software Amira 6.7 (Thermo Fisher Scientific, MA, USA). The length of each segment was determined by summing the Euclidean distances between adjacent points in the respective segment; the segments' tortuosity was then calculated by dividing the true length by the chord length—defined as the shortest distance between the start and end points of the segment. Additionally, the total numbers of segments and nodes together with the number of branching

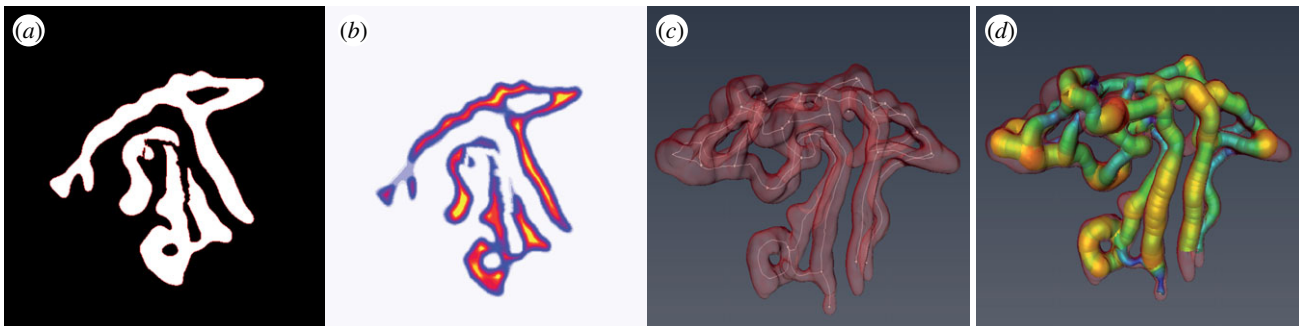


Figure 1. (a) A typical segmented stack. (b) Respective distance map where yellow is far and purple is near. (c) Skeleton of the vascular network (white). (d) Radius estimation representation. (Online version in colour.)

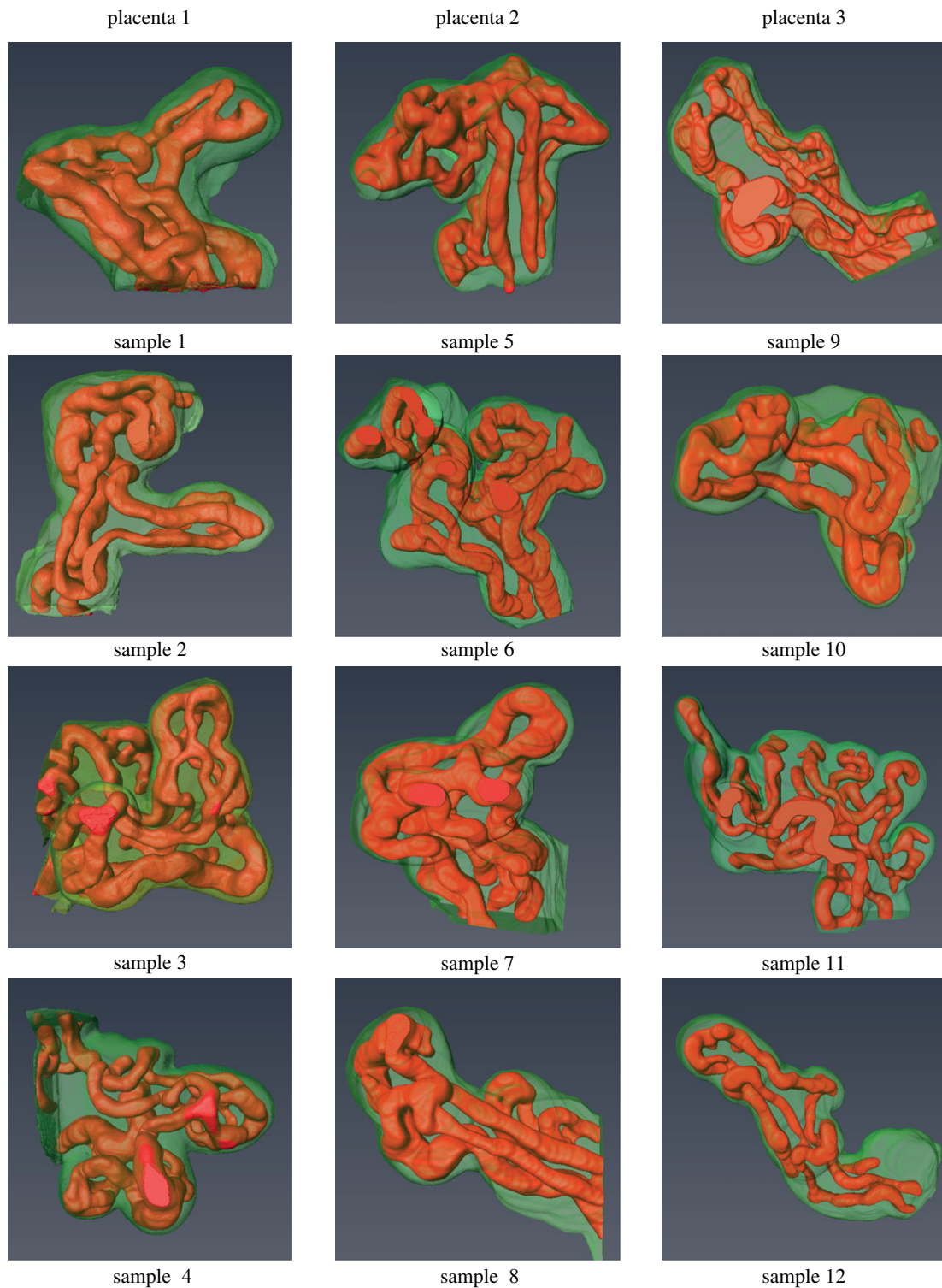


Figure 2. Three-dimensional reconstructions of the 12 samples showing the villous membrane (green) and the capillary network (red). (Online version in colour.)

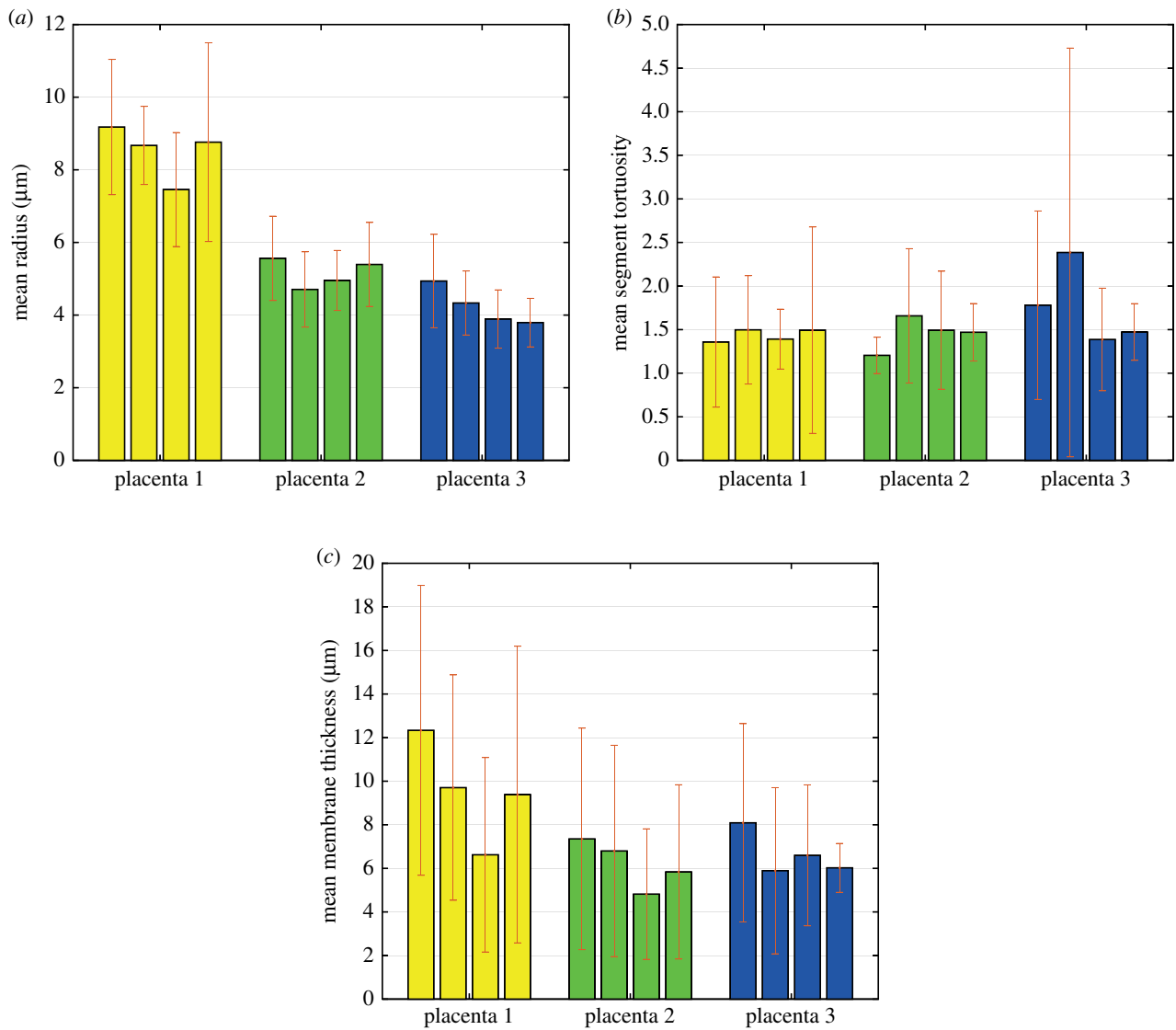


Figure 3. Arithmetic mean values of capillary radius (a), branch tortuosity (b) and barrier thickness (c) with their respective deviation of all samples and grouped by placenta. (Online version in colour.)

nodes were automatically provided by the software. The branching nodes were then manually sorted into a bifurcation node if it contained three connected segments or trifurcation node if it included four segments. The vascular network degree of connectivity was measured by the beta index [31], defined as the number of segments divided by the number of nodes; this measure gives an estimation of the density of connections which can be translated into how robust a transportation network is—a higher beta index indicates on a more efficient network. The surface area and volume of the samples were obtained by employing the *Surface Area Volume* module. Volume and surface area fractions between the capillaries and villous membrane were then calculated. In order to obtain the villous membrane thickness, the shortest distance from the fetoplacental capillary skeleton to the membrane border was estimated by evaluating the membrane distance map on the vessels' centreline. Afterwards, the capillary radius was subtracted.

Average values per sample, per placenta and averaging of the entire available data were calculated using the arithmetic mean (equation (2.1)). The samples' standard deviation (equation (2.2)) and the harmonic mean (equation (2.3)) of the villous membrane thickness were also calculated. The uniformity index, defined as the ratio between the arithmetic and harmonic means [32], was then estimated. Arithmetic mean, harmonic mean and standard deviation were calculated in Matlab R2018a (Mathworks, MA, USA); statistical analyses

were performed in GraphPad Prism (GraphPad Software, CA, USA) and determined by the D'Agostino–Pearson test [33],

$$X = \frac{1}{n} \sum_{i=1}^n x_i, \quad (2.1)$$

$$\sqrt{\frac{\sum_{i=1}^n (x_i - X)^2}{(n-1)}} \quad (2.2)$$

and

$$H = \left(\frac{\sum_{i=1}^n x_i^{-1}}{n} \right)^{-1}. \quad (2.3)$$

3. Results

Twelve terminal villi were successfully reconstructed from the CLSM image stacks (figure 2). There is considerable variation in the complexity of the samples, showing the wide range of capillary arrangements that exist among terminal villi.

The mean capillary radius, segment tortuosity and membrane thickness are plotted in figure 3 per specimen and grouped by placenta. The mean radius was higher in the first placenta than in the other two, but there is no statistically significant difference between the placentas ($p > 0.05$); it must be remembered that the number of samples in each placenta (four) was small. It is also noticeable that the mean radius was almost constant per placenta (figure 3a), suggesting that

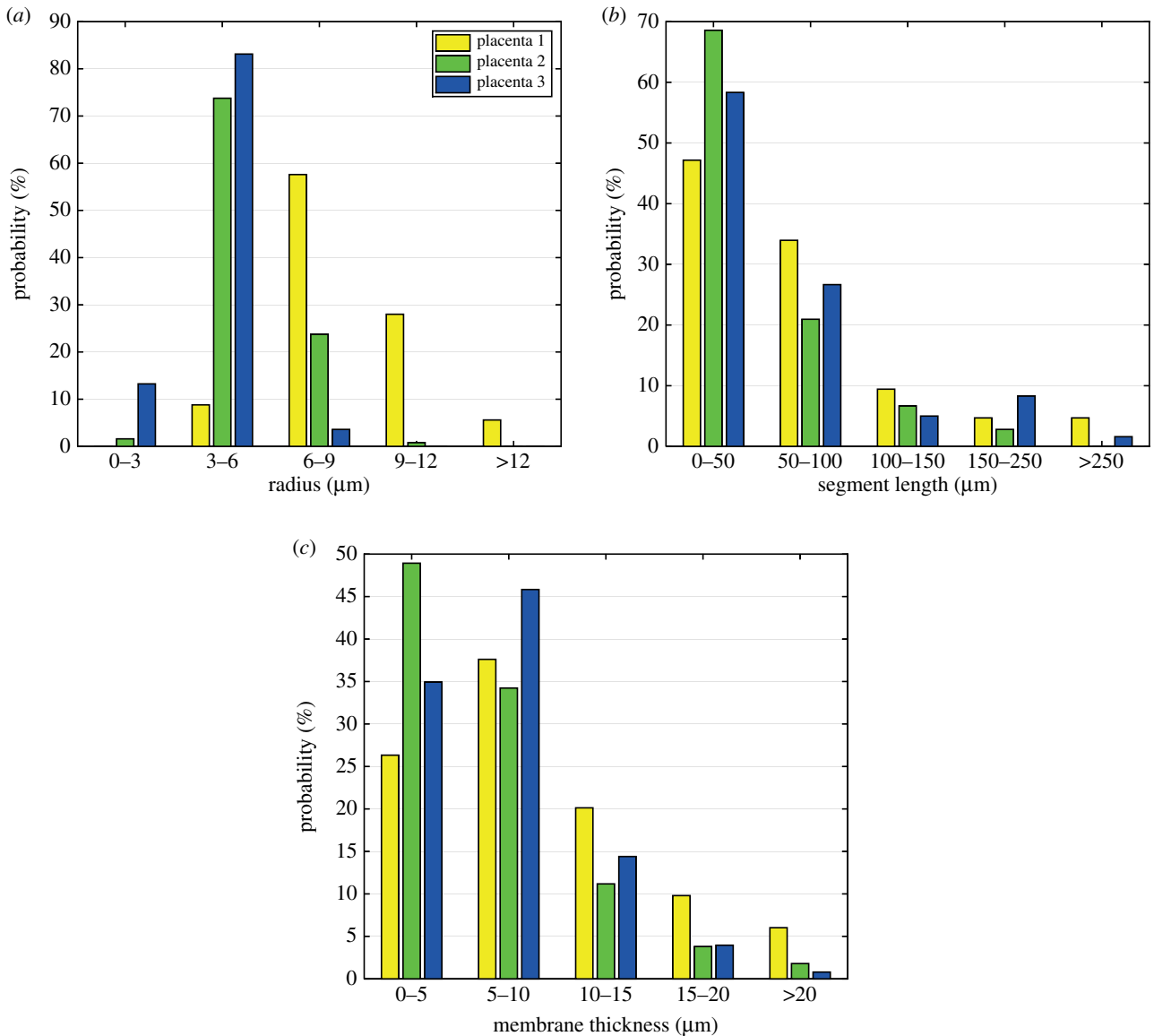


Figure 4. Distribution of vessel radius, branch length and membrane thickness per placenta. (Online version in colour.)

there is an inter-individual variation rather than a disparity between samples. The mean segment tortuosity was similar within and between placentas (figure 3*b*), with all the samples showing significant curvature. The arithmetic mean membrane thickness also appears to be similar in each placenta, and with no significant difference between them ($p > 0.05$; figure 3*c*). On the other hand, the mean barrier thickness shows large deviations due to the marked difference between the thin and thick areas; this is best demonstrated in figure 4*c*.

Figure 4 shows the distribution of values for the capillary radius, segment lengths and membrane thicknesses grouped per placenta. The fetio-capillary radius shows a normal distribution ($p < 0.001$) with most of them between 3 and 9 μm (figure 4*a*) and almost no probability of having a radius above 12 μm . A large proportion of the capillary segments are shorter than 100 μm , but no longer than 250 μm (figure 4*b*). Additionally, from figure 4*c*, it can be appreciated that approximately 35% of the membrane thicknesses are thinner than 5 μm with fewer than 5% thicker than 15 μm .

Tables 1 and 2 summarize all the results. The mean vessel radius and length were $6.17 \pm 2.41 \mu\text{m}$ and $61.09 \pm 55.21 \mu\text{m}$,

respectively. The standard deviation of the segment lengths ($\pm 55.21 \mu\text{m}$) was high, suggesting that the vessels are considerably irregular. The tortuosity values show that the vessels are curved with all the specimens having values larger than 1. The arithmetic and harmonic mean barrier thicknesses ($7.5 \pm 2.1 \mu\text{m}$ and $4.5 \pm 1.8 \mu\text{m}$, respectively) were significantly different ($p < 0.005$); this is best reflected in the values of the large uniformity index, which were on average 1.62. This parameter is a good indicator of the proportion of the villous surface formed by vasculo-syncytial membranes [1].

Finally, an analysis of the fetio-capillary system as a transport network was performed (table 2). Most of the branching points were bifurcation nodes (91.8%) with only a few trifurcation branching nodes (8.2%). The beta index was on average 1.2 and was always above 1; this indicates that the system is a very efficient network for transport purposes because it includes more than one closed path. The capillary to villus volume fraction and surface area ratio were $21.04 \pm 5.05\%$ and 0.92 ± 0.13 , respectively. The average surface fraction in placenta 2 was above 1, but there was no statistically significant difference ($p > 0.005$) when compared with the other placentas.

Table 1. Details of some parameters per sample, per placenta and for all the data. No significant difference was found between placentas ($p > 0.05$).

	segment length (μm)	segment tortuosity	segment radius (μm)	membrane thickness (μm)	harmonic thickness (μm)	uniformity index
sample 1	66.64	1.36	9.18	12.33	8.37	1.47
sample 2	142.40	1.50	8.67	9.70	7.14	1.36
sample 3	75.89	1.39	7.46	6.62	2.70	2.45
sample 4	59.93	1.49	8.76	9.39	3.50	2.68
placenta 1	72.13 \pm 66.35	1.42 \pm 0.81	8.47 \pm 2.13	9.51 \pm 2.34	5.43 \pm 2.75	1.75 \pm 0.67
sample 5	35.48	1.20	5.56	7.35	5.05	1.47
sample 6	65.77	1.66	4.71	6.80	2.53	2.68
sample 7	40.01	1.49	4.95	4.82	2.86	1.68
sample 8	45.48	1.47	5.39	5.84	3.83	1.52
placenta 2	48.62 \pm 39.08	1.43 \pm 0.55	5.20 \pm 1.13	6.20 \pm 1.11	3.57 \pm 1.13	1.74 \pm 0.57
sample 9	91.54	1.78	4.94	8.09	5.17	1.57
sample 10	91.08	2.39	4.33	5.89	3.65	1.62
sample 11	38.78	1.39	3.89	6.60	5.09	1.30
sample 12	101.87	1.47	3.79	6.02	4.99	1.21
placenta 3	62.80 \pm 53.83	1.63 \pm 1.16	4.15 \pm 0.99	6.65 \pm 1.01	4.72 \pm 0.72	1.41 \pm 0.20
total	61.09 \pm 55.21	1.48 \pm 0.84	6.17 \pm 2.41	7.45 \pm 2.11	4.57 \pm 1.79	1.63 \pm 1.18
p	>0.05	>0.05	>0.05	>0.05	>0.05	>0.05

Table 2. Details of some parameters per sample, per placenta and for all the data.

	bifurcations	trifurcations	beta index	volume fraction (%)	surface ratio
sample 1	20	2	1.46	28	1.05
sample 2	6	1	1.08	25	0.82
sample 3	21	1	1.27	21	0.78
sample 4	23	1	1.41	21	0.89
placenta 1	70 ^a	5 ^a	1.30	23.75	0.89
	93.33%	6.66%	\pm 0.17	\pm 3.40	\pm 0.12
sample 5	25	3	1.42	18.68	1.03
sample 6	22	0	1.31	20.45	0.98
sample 7	9	1	1.12	23.90	1.13
sample 8	12	2	1.44	30.80	1
placenta 2	68 ^a	6 ^a	1.32	23.46	1.04
	91.89%	8.10%	\pm 0.15	\pm 5.36	\pm 0.07
sample 9	10	0	1.33	16.70	0.93
sample 10	5	2	1.30	15.43	0.88
sample 11	22	3	1.18	16.49	0.92
sample 12	4	0	1.00	15.06	0.64
placenta 3	41 ^a	5 ^a	1.20	15.99	0.84
	89.13%	10.86%	\pm 0.15	\pm 0.80	\pm 0.13
total	179 ^a	16 ^a	1.20	21.04	0.92
	91.8%	8.2%	\pm 0.06	\pm 5.05	\pm 0.13
p			>0.05	>0.05	>0.05

^aThese values are the totals.

Table 3. Published morphological findings of human placental terminal villi.

fixation technique	quantification technique	reference	volume fraction (%)	surface ratio	mean membrane thickness (μm)	harmonic	vessel diameter (μm)
						membrane thickness (μm)	
<i>in situ</i> biopsy	semithin sections	Sen <i>et al.</i> [6]	35 ± 8.01	0.92 ± 0.35	4.25		
<i>in situ</i> biopsy	vessel cast	Kauffman <i>et al.</i> [7]					12.30
<i>in situ</i> biopsy	semithin sections	Kauffman <i>et al.</i> [7]					14.50
perfusion	semithin sections	Burton <i>et al.</i> [1]	39.39 ± 3.81	1.35 ± 0.07	4.84 ± 0.50	3.63 ± 0.42	20.75 ± 1.86
immersion	semithin sections	Burton <i>et al.</i> [1]	25.90 ± 5.62	1.13 ± 0.15	6.03 ± 0.64	4.87 ± 0.66	13.97 ± 2.25
perfusion	vessel cast	Krebs <i>et al.</i> [11]					12.7 ± 3.80
immersion	semithin sections	Mayhew <i>et al.</i> [16]	29 ± 0.03	0.94 ± 0.09			
perfusion	3D reconstructions	current study	21.04 ± 5.05	0.92 ± 0.13	7.45 ± 2.11	4.57 ± 1.79	12.3 ± 2.41

4. Discussion

The morphology of the terminal villi and of the fetoplacental vessels is of major interest due to their critical role in the transport of gases, nutrients and waste products between the maternal and fetal circulations. Inadequate development of the terminal villi has been broadly shown to be related with pregnancy complications [3,11–22] and, therefore, a deeper understanding of the spatial arrangement of the villi is key to better assessing placental pathologies. The current study was designed to improve our understanding of the architecture and morphological features of the terminal villi using 3D reconstructions of perfused placentas. Three-dimensional reconstruction of fluorescent CLSM images is emerging as a potential technique to analyse more extensively the terminal villi since it slices the tissue virtually with high resolution, especially when compared with standard paraffin-embedded sections [24–27]. Our results show that this approach is able to capture the complex architecture of the fetoplacental capillaries, their varying diameters and loops (figure 2). If the vessels are reconstructed together with the villous membrane, this method can also accurately calculate the extent and thickness of the vasculo-syncytial membranes.

Characteristic parameters of the terminal villi have been widely investigated using different fixation techniques such as: *in situ* biopsy [5–7], perfusion and immersion fixation [1,16,26], together with different imaging and quantitative approaches as stereology [1,5,16], 3D vascular casts [7,11] and 3D CLSM reconstructions [24–27]; table 3 summarizes the published data. The results of this study show that the perfusion pressure does not have a significant impact on the structural parameters; this is best seen in figure 3, where the mean radius, tortuosity and membrane thickness are similar for all the samples in placenta 1. Consequently, the perfusion pressure should be the one that allows free perfusate flow and avoids vascular damage. Our data are in excellent agreement with those of Sen *et al.* [6] and Kaufman *et al.* [5,7] (see surface ratio and vessel diameter, table 3), who aspirated villi directly into fixative from the placenta still *in situ* at the time of a caesarean section, and with Krebs *et al.* [11], who created 3D vessel casts from perfused lobules. Volume fractions and membrane thickness were notably different when compared with those previously reported by Burton *et al.* [1] for perfused placentas, but are in agreement with those reported for immersion fixation by the same authors [1]. Interestingly, our results

showed that there is an inter-individual variation rather than a significant variability within a placenta (figure 4 and table 2), suggesting that some of the marked differences from the data published by Burton *et al.* [1] might be attributed to the natural diversity of women. Additionally, it is worth noting that membrane thicknesses are 3D measurements which cannot be accurately estimated from planar 2D images.

Harmonic mean thickness has been regarded as the physiologically important parameter for accurate estimation of the diffusive capacity in exchange organs [1,34]. This is because in systems where the separating barrier varies considerably, such as the placenta, the thin areas have a critical role in enhancing transport. Figure 4 shows that approximately half of the villous membrane is thinner than $6 \mu\text{m}$, in agreement with Sen *et al.* [6] and supporting the use of the harmonic mean thickness. An alternative parameter for the estimation of the extent of the vasculo-syncytial membranes is the uniformity index (table 1); the high value measured here compared with that reported by Burton *et al.* [1] (1.63 ± 1.18 versus 1.34 ± 0.009) demonstrates that the proposed technique is more sensitive to the irregularities of the vessels' diameter.

Some new parameters have been introduced for the first time in this study in an attempt to describe the 3D architecture of the fetoplacental capillary network and its efficiency as a means of transport. From table 2, it is clear that the vessels in the terminal villi generally divide into two daughter branches (91.8%) rather than three (8.2%); however, trifurcations were found in most of the samples, suggesting that this phenomenon is not uncommon. Additionally, from table 1, it can be appreciated that the branches are highly tortuous, a common manoeuvre to extend length, increase surface area and slow blood flow to allow longer duration for transport processes. Lastly, the beta index (table 2) is a simple measure of a network's degree of connectivity since it provides an approximation of the density of connections; values above 1 indicate several paths while a value of exactly 1 suggests a system with only one path, such as sample 12. The fact that all but one sample have a beta index higher than 1 means that the capillary networks are very efficient for transport purposes, providing several different circuits for the blood to flow through. This might be a beneficial way of maximizing transport, allowing blood to re-circulate and absorb any remaining nutrients.

Although the proposed approach has many obvious advantages, it does possess some limitations. Technical problems related to the need to immediately perfuse placental

lobules after delivery, fluorescent staining and CLSM imaging have been previously documented [10]. Additionally, the segmentation of CLSM needs an experienced user who is familiar with the topology of the terminal villi in order to identify image artefacts. Recently, clarification of immunolabelled villi has been shown to improve the image quality, and is expected to ease the segmentation process [35,36]. Lastly, there are statistical limitations due to the sample size, which, while it is representative, might have not captured all the variability existing within and between placentas.

5. Conclusion

Morphological analysis of the terminal villi and their capillary beds has been of interest for a long time, due to their key role in transporting nutrients and waste products between the maternal and fetal circulations. Previous techniques were limited by fixation and imaging approaches. The current study used 3D reconstructions from perfused

placentas to better quantify and analyse terminal villous architecture and spatial characteristics. The proposed technique was able to accurately capture the irregularities in the vessel diameter and membrane thickness that are often lost in physical sectioning and 2D imaging. This approach can become a robust tool to characterize placental differences in pregnancy complications and between different populations.

Data accessibility. This article has no additional data.

Authors' contributions. R.P.M., D.S.C.J., G.J.B. and G.M. contributed to the design of the study and preparation of the manuscript. R.P.M. performed all the reconstructions and data analyses. Y.A. was involved in the samples' preparation and imaging. All authors revised and agree on the submitted manuscript.

Competing interests. The authors confirm that there were no conflicts of interest associated with the funding or conduct of this work.

Funding. This project was funded by the Centre for Trophoblast Research (CTR), University of Cambridge, Cambridge, UK.

Acknowledgements. The authors would like to thank Dr Tereza Cindrova-Davies for her help with the samples' preparation and useful comments.

References

- Burton GJ, Ingram SC, Palmer ME. 1987 The influence of mode of fixation on morphometrical data derived from terminal villi in the human placenta at term: a comparison of immersion and perfusion fixation. *Placenta* **8**, 37–51. (doi:10.1016/0143-4004(87)90038-5)
- Mayhew TM. 2009 A stereological perspective on placental morphology in normal and complicated pregnancies. *J. Anat.* **215**, 77–90. (doi:10.1111/joa.2009.215.issue-1)
- Macara L, Kingdom JCP, Kaufmann G, Kohlen P, Hair J, More IAR, Lyall F, Greer IA. 2007 Structural analysis of placental terminal villi from growth-restricted pregnancies with abnormal umbilical artery doppler waveforms. *Placenta* **78**, 37–48. (doi:10.1016/s0143-4004(05)80642-3)
- Mayhew TH, Joy CF, Haas JD. 1984 Structure-function correlation in the human placenta, the morphometric diffusing capacity for oxygen at full term. *J. Anat.* **139**, 691–708.
- Kaufmann P, Sen D, Schweikhart G. 1979 Classification of human placental villi. *Cell Tissue Res.* **200**, 409–423. (doi:10.1007/BF00234852)
- Sen D, Kaufmann P, Schweikhart G. 1979 Classification of human placental villi. *Cell Tissue Res.* **200**, 425–434. (doi:10.1007/BF00234853)
- Kaufmann P, Bruns U, Leiser R, Luckhardt M, Winterhager E. 1985 The fetal vascularisation of term human placental villi. II. Intermediate and terminal villi. *Anat. Embryol.* **173**, 203–214. (doi:10.1007/BF00316301)
- Burton GJ. 1986 Scanning electron microscopy of intervillous connections in the mature human placenta. *J. Anat.* **147**, 245–254.
- Burton G. 1987 The fine structure of the human placental villus as revealed by scanning electron microscopy. *Scanning Microsc.* **1**, 1811–1828.
- Plitman Mayo R, Charnock-Jones DS, Burton GJ, Oyen ML. 2016 Three-dimensional modeling of human placental terminal villi. *Placenta* **43**, 54–60. (doi:10.1016/j.placenta.2016.05.001)
- Krebs C, Macara LM, Leiser R, Bowman AW, Greer IA, Kingdom JC. 1995 Intrauterine growth restriction with absent end-diastolic flow velocity in the umbilical artery is associated with maldevelopment of the placental terminal villous tree. *Am. J. Obstet. Gynecol.* **6**, 1534–1542. (doi:10.1016/s0002-9378(96)70103-5)
- Honda M, Toyoda C, Nakabayashi M, Omori Y. 1992 Quantitative investigations of placental terminal villi in maternal diabetes mellitus by scanning and transmission electron microscopy. *Tohoku J. Exp. Med.* **167**, 247–257. (doi:10.1620/tjem.167.247)
- Almasy SM, Elfayomy AK. 2012 Morphometric analysis of terminal villi and gross morphological changes in the placenta of term idiopathic intrauterine growth restriction. *Tissue Cell* **44**, 214–219. (doi:10.1016/j.tice.2012.03.006)
- Ansari T, Fenlon S, Pasha S, O'Neill B, Gillan J, Green C, Sibbons P. 2003 Morphometric assessment of the oxygen diffusion conductance in placenta from pregnancies complicated by intra-uterine growth restriction. *Placenta* **24**, 618–626. (doi:10.1016/S0143-4004(03)00044-4)
- Mayhew TM, Ohadike C, Baker PN, Crocker IP, Mitchell C, Ong SS. 2003 Stereological investigation of placental morphology in pregnancies complicated by pre-eclampsia with and without intrauterine growth restriction. *Placenta* **24**, 219–226. (doi:10.1053/plac.2002.0900)
- Mayhew TM, Wijesekera J, Baker PN, Ong SS. 2004 Morphometric evidence that villous development and fetoplacental angiogenesis are compromised by intrauterine growth restriction but not by pre-eclampsia. *Placenta* **25**, 829–833. (doi:10.1016/j.placenta.2004.04.011)
- Mayhew TM, Sisley I. 1998 Quantitative studies on the villi, trophoblast and intervillous pores of placenta from women with well-controlled diabetes mellitus. *Placenta* **19**, 371–377. (doi:10.1016/S0143-4004(98)90076-5)
- Calderon IMP, Damasceno DC, Amorin RL, Costa RAA, Brasil MAM, Rudge MVC. 2007 Morphometric study of placental villi and vessels in women with mild hyperglycemia or gestational or overt diabetes. *Diabetes Res. Clin. Pract.* **78**, 65–71. (doi:10.1016/j.diabetes.2007.01.023)
- Egbor M, Ansari T, Morris N, Green CJ. 2006 Morphometric placental villous and vascular abnormalities in early- and late-onset pre-eclampsia with and without fetal growth restriction. *BJOG: Int. J. Obstet. Gynaecol.* **113**, 580–589. (doi:10.1111/j.1471-0528.2006.00882.x)
- Resta L, Capobianco C, Marzullo A, Piscitelli D, Sanguedolce F, Schena FP, Gesualdo L. 2006 Confocal laser scanning microscope study of terminal villi vessels in normal term and pre-eclamptic placentas. *Placenta* **27**, 735–739. (doi:10.1016/j.placenta.2005.07.006)
- Sankar KD, Bhanu PS, Kiran S, Ramakrishna BA, Shanthi V. 2012 Vasculosyncytial membrane in relation to syncytial knots complicates the placenta in preeclampsia: a histomorphometrical study. *Anat. Cell Biol.* **45**, 86–91. (doi:10.5115/ach.2012.45.2.86)
- Bhanu PS, Sankar KD, Swetha M, Kiran S, Devi S. 2016 Morphological and micrometrical changes of the placental terminal villi in normal and pregnancies complicated with gestational diabetes mellitus. *Evid. Based Med. Healthc.* **3**, 2349–2562.
- Jirkovská M *et al.* 2012 The branching pattern of villous capillaries and structural changes of

- placental terminal villi in type 1 diabetes mellitus. *Placenta* **33**, 343–351. (doi:10.1016/j.placenta.2012.01.014)
24. Jirkovská M. 2002 Topological properties and spatial organization of villous capillaries in normal and diabetic placentas. *J. Vasc. Res.* **39**, 268–278. (doi:10.1159/000063692)
25. Jirkovská M, Janáček J, Kaláb J, Kubínová L. 2008 Three-dimensional arrangement of the capillary bed and its relationship to microrheology in the terminal villi of normal term placenta. *Placenta* **29**, 892–897. (doi:10.1016/j.placenta.2008.07.004)
26. Plitman Mayo R, Charnock-Jones SD, Burton GJ, Oyen ML. 2014 3D surface reconstruction of human terminal villi and the fetal capillary bed. *Placenta* **35**, A8–A9. (doi:10.1016/j.placenta.2014.06.030)
27. Plitman Mayo R, Olsthoorn J, Charnock-Jones SD, Burton GJ, Oyen ML. 2016 Computational modeling of the structure-function relationship in human placental terminal villi. *J. Biomech.* **49**, 3780–3787. (doi:10.1016/j.jbiomech.2016.10.001)
28. Haeussner E *et al.* 2015 Does 2D-histologic identification of villous types of human placentas at birth enable sensitive and reliable interpretation of 3D structure. *Placenta* **36**, 1425–1432. (doi:10.1016/j.placenta.2015.10.003)
29. Plitman Mayo R. 2018 Advances in human placental biomechanics. *Comput. Struct. Biotechnol. J.* **16**, 298–306. (doi:10.1016/j.csbj.2018.08.001)
30. Shapiro LG, Stockman GC 2002 *Computer vision*. Englewood Cliffs, NJ: Prentice Hall.
31. Levinson D. 2012 Network structure and city size. *PLoS ONE* **7**, e29721. (doi:10.1371/journal.pone.0029721)
32. Jackson MR, Joy CF, Mayhew TM, Hass JD. 1985 Stereological studies on the true thickness of the villous membrane in human term placentae: a study of placentae from high-altitude pregnancies. *Placenta* **6**, 249–258. (doi:10.1016/S0143-4004(85)80054-0)
33. D'Agostino RB 1986 *Goodness-of-fit techniques*. New York, NY: Marcel Dekker.
34. Weibel ER, Knight BW. 1964 A morphometric study on the thickness of the pulmonary air-blood barrier. *J. Cell Biol.* **21**, 367–384. (doi:10.1083/jcb.21.3.367)
35. Merz G, Schwenk V, Shah R, Necaise P, Salafia CM. 2017 Clarification and 3D visualization of immunolabeled human placenta villi. *Placenta* **53**, 36–39. (doi:10.1016/j.placenta.2017.03.015)
36. Merz G, Schwenk V, Shah R, Salafia CM, Necaise P, Joyce M, Villani T, Johnson M, Crider N. 2017 Clarification and 3D visualization of immunolabeled human placenta villi. *Placenta* **53**, 36–39. (doi:10.1016/j.placenta.2017.03.015)